

The Crucial Role and an Effective Modulation Method of Intermolecular π - π Interaction of the Well-known A-D-A Type Electron Acceptor

Bowei Gao, Huifeng Yao*, Bomee Jang, Jie Zhu, Runnan Yu, Yong Cui, Fenghao Wang, Junxian Hou*, Han Young Woo*, and Jianhui Hou*

B. Gao, Dr. H. Yao, J. Zhu, R. Yu, Y. Cui, F. Wang, Prof. J. Hou

State Key Laboratory of Polymer Physics and Chemistry, Beijing National Laboratory for Molecular Sciences, CAS Research/Education Center for Excellence in Molecular Sciences, Institute of Chemistry, Chinese Academy of Sciences, Beijing 100190, China.

E-mail: yaohf@iccas.ac.cn; hjhzlz@iccas.ac.cn

B. Jang, Prof. H. Y. Woo

Department of Chemistry, Korea University, Seoul 136-701, Republic of Korea.

E-mail: hywoo@korea.ac.kr

Dr. J. Hou

Department of Composite Materials and Engineering College of Materials Science and Engineering Hebei University of Engineering Handan 056038, P. R. China

E-mail: houjx@iccas.ac.cn

B. Gao, R. Yu, Y. Cui, Prof. J. Hou

University of Chinese Academy of Sciences, Beijing 100049, China.

Contents

Experiment section	3
Instruments and Measurements	3
S1. NMR spectra of the target products	3
S2. TGA	5
S3. Films of acceptors spin coated by CB	5
S4. Theoretical study	6
S5. Optimized dimer geometries	6
Table S1. Summary of photovoltaic parameters of the PBDB-T:ITCC-based OSC devices with different D:A ratios and DIO contents.	7
S6. Absrption properties of acceptors	7
S7. Electron mobilities of pure acceptor films	7
S8. Charge recombination properties	8
S9. Hole mobilities of blended films.....	8
S10. Morphology of blended films	8
References.....	9

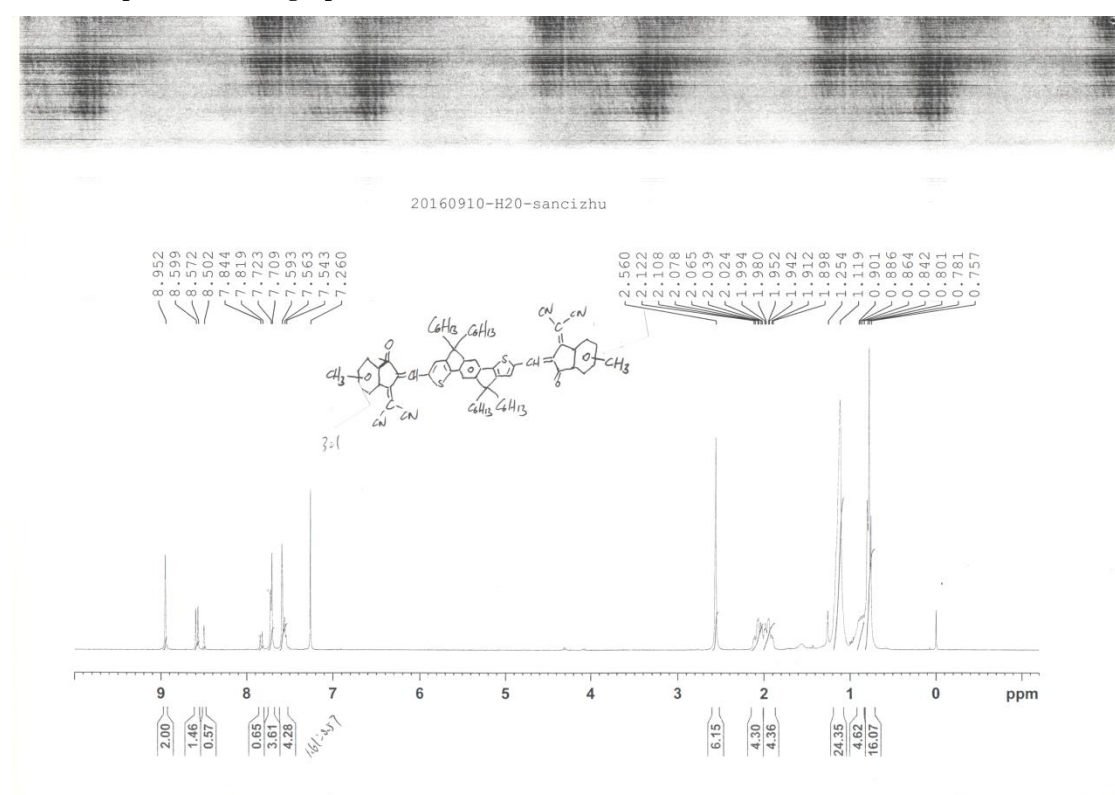
Experiment section

Instruments and Measurements

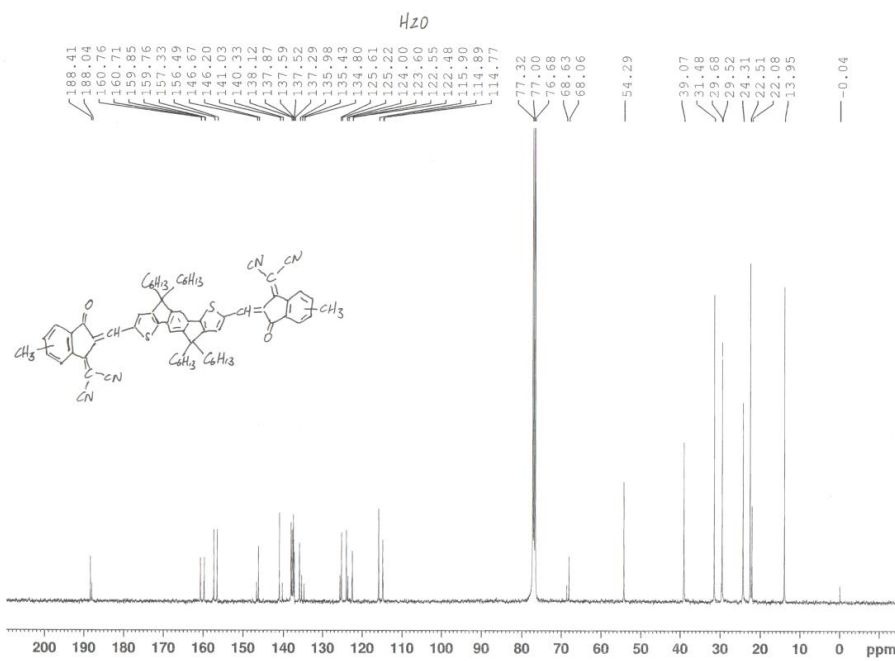
Bruker AVANCE 300 or 400 MHz spectrometer was used to measure the ^1H and ^{13}C NMR spectra of the compounds in the synthetic procedure at room temperature. Absorption spectra (in chloroform solution and as thin films) and molecular energy levels of the small molecular acceptors were measured on a Hitachi UH4150 UV-Vis spectrophotometer and a CHI650D Electrochemical Workstation, respectively. In the molecular energy level measurements, 0.1 M Bu_4NPF_6 acetonitrile solution was used as electrolyte, and ferrocene/ferrocenium was used as external standard and measured in parallel. The thickness of blend layers was measured via the surface profilometer Bruker Dektak XT. AFM and TEM images were obtained by Nanoscope V AFM and JEOL 2200FS instrument, respectively. The electron mobility was measured by SCLC method,¹ and the equations of $J = (9/8)\varepsilon_0\varepsilon_r\mu_e V^2/L^3$ was used to calculate the electron mobility, where ε_0 is the permittivity of free space, ε_r is the relative permittivity of the organic material, μ is the electron mobility, V_{app} is the effective applied voltage, and L is the thickness of the film.

Morphology Characterizations: GIWAXS measurements were conducted at the PLS-II 9A U-SAXS beam line of Pohang Accelerator Laboratory. The photo-CELIV measurements reported here were performed by the all-in-one characterization platform Paios developed and commercialized by Fluxim AG, Switzerland, the under a 0.32 V/us linearly increasing reverse bias pulse.²

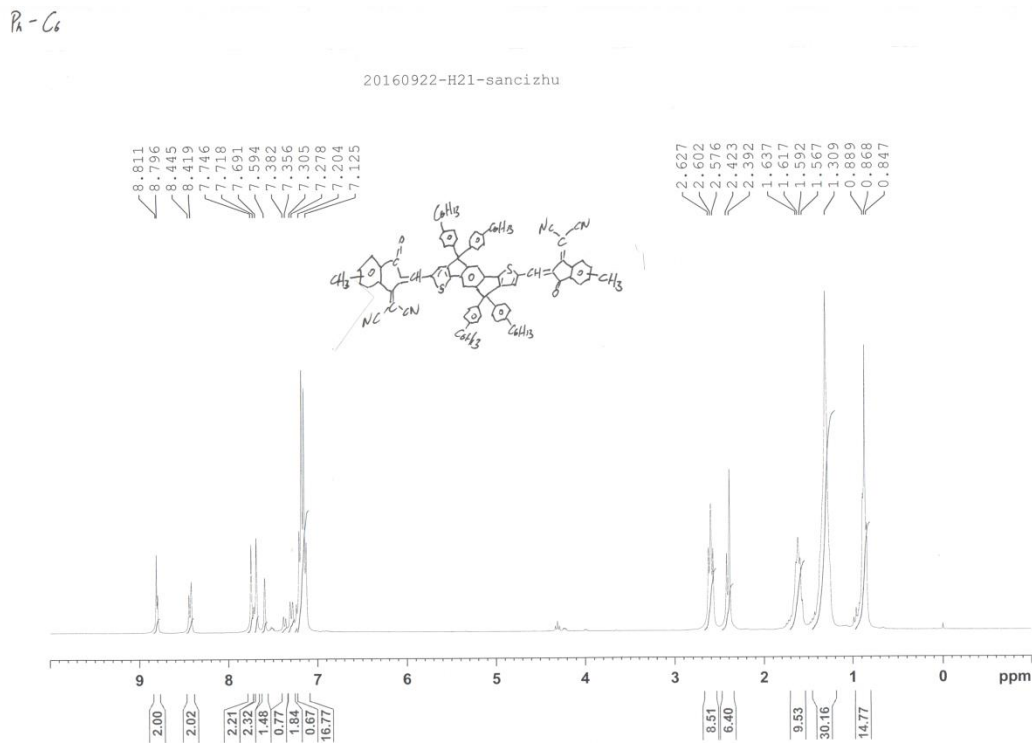
S1. NMR spectra of the target products



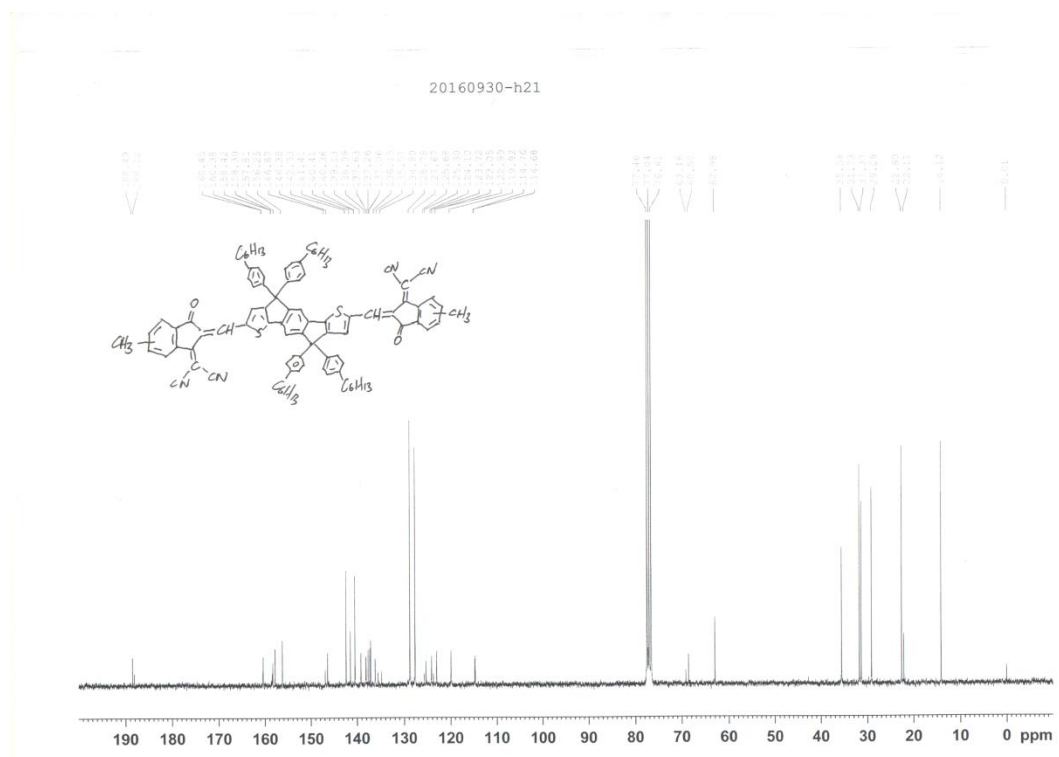
^1H NMR spectrum of IDT-C6



^{13}C NMR spectrum of IDT-C6



^1H NMR spectrum of IDT-PhC6



¹³C NMR spectrum of IDT-PhC6

Figure S1. NMR spectra of the target products.

S2. TGA

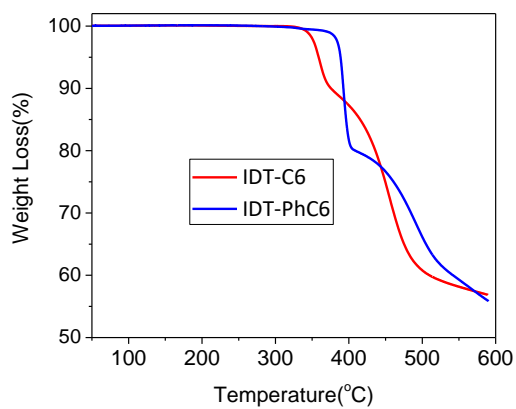


Figure S2. TGA plots of IDT-C6 and IDT-PhC6.

S3. Films of acceptors spin coated by CB



Figure S3. Photos of IDT-C6 and IDT-PhC6 films in chlorobenzene, captured by the camera of the surface profilometer Bruker Dektak XT.

S4. Theoretical study

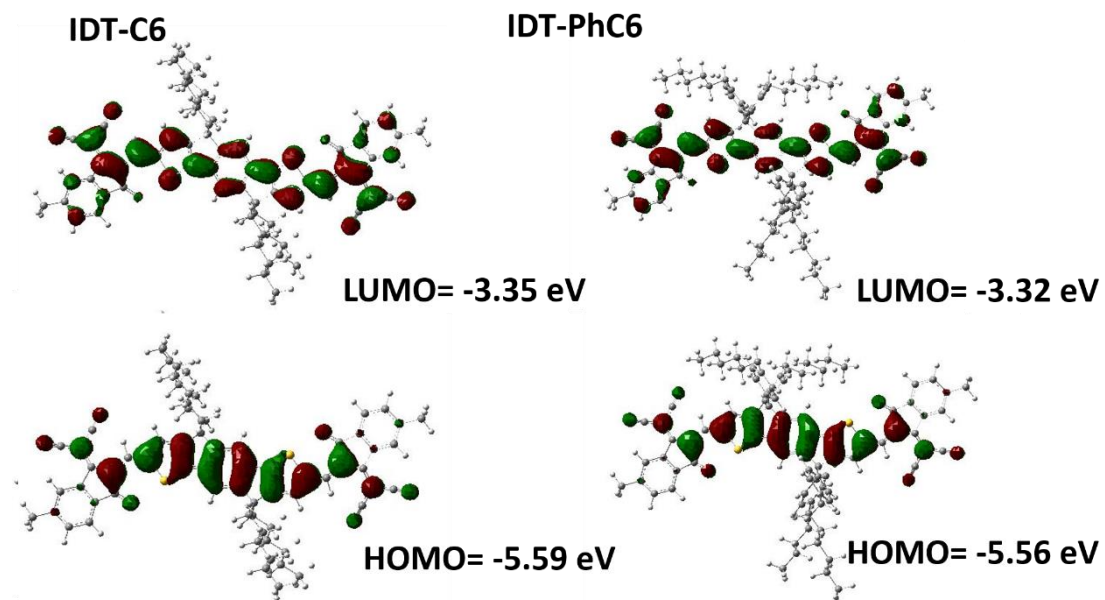


Figure S4. Optimized molecular geometries and frontier molecular orbitals for IDT-C6 and IDT-PhC6 calculated by DFT at the B3LYP/6-31G(d, p) level.

S5. Optimized dimer geometries

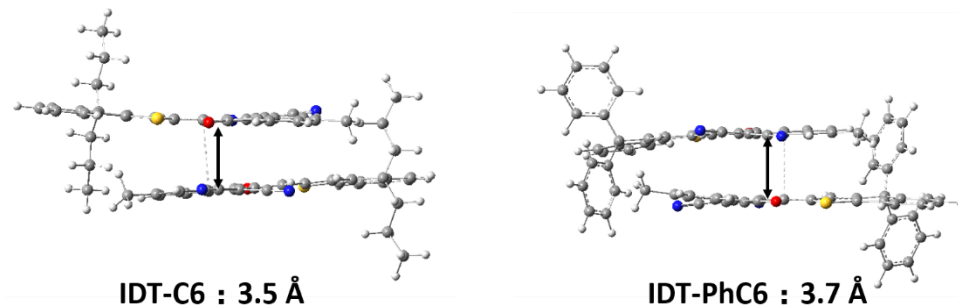


Figure S5. Optimized dimer geometries for IDT-C6 and IDT-PhC6.

Devices	D:A	DIO (v/v)	V_{oc} (V)	J_{sc} (mA/cm ²)	FF	PCE (%)
	1.5:1	none	0.96	16.6	0.63	10.0
	1:1	none	0.96	16.8	0.66	10.6
PBDB-TF: IDT-C6	1:1.5	none	0.96	15.7	0.64	9.6
	1:1	0.5%	0.96	17.5	0.74	12.5

1:1	1%	0.95	15.9	0.71	10.7
1:1	2%	0.95	12.1	0.64	7.35

Devices	D:A	DIO (v/v)	V_{oc} (V)	J_{sc}	FF (%)	PCE (%)
				(mA/cm ²)		
PBDB-TF:IDT- PhC6	1.5:1	none	0.99	11.5	0.41	4.7
	1:1	none	1.00	12.0	0.41	4.9
	1:1.5	none	1.00	12.4	0.37	4.6
	1:1	0.5%	1	12.1	0.43	5.2
	1:1	1%	0.99	11.7	0.41	4.7
	1:1	2%	0.99	10.4	0.37	3.8

Table S1. Summary of photovoltaic parameters of the PBDB-T:ITCC-based OSC devices with different D:A ratios and DIO contents.

S6. Absorption properties of acceptors.

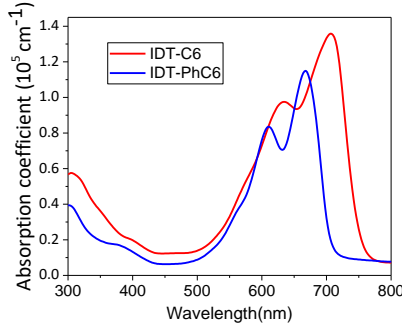


Figure S6. Absorption spectra of IDT-C6 and IDT-PhC6 films.

S7. Electron mobilities of pure acceptor films

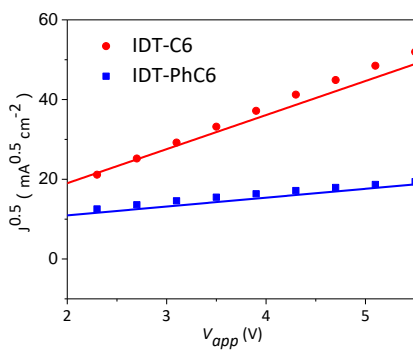


Figure S7. $J^{0.5}$ -V plots of IDT-C6 and IDT-PhC6 based electron-only device.

S8. Charge recombination properties

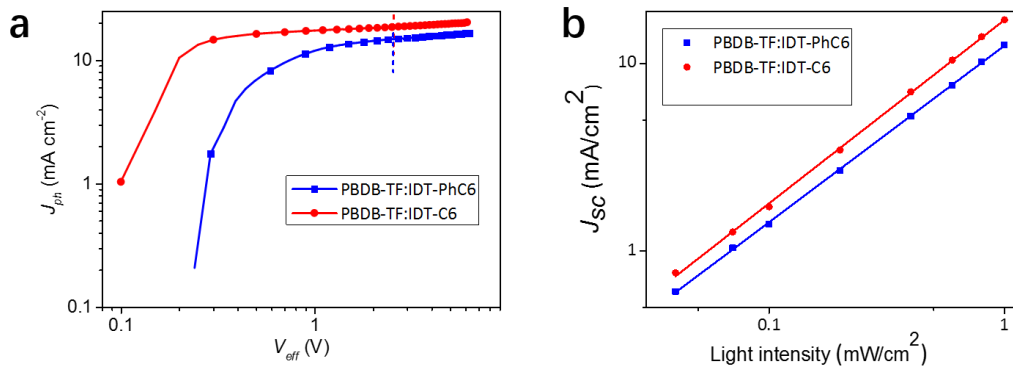


Figure S8. a) J_{ph} versus V_{eff} of the optimized devices. b) Photocurrent dependence on the light intensity for the IDT-C6- and IDT-PhC6-based OSC devices.

S9. Hole mobilities of blended films

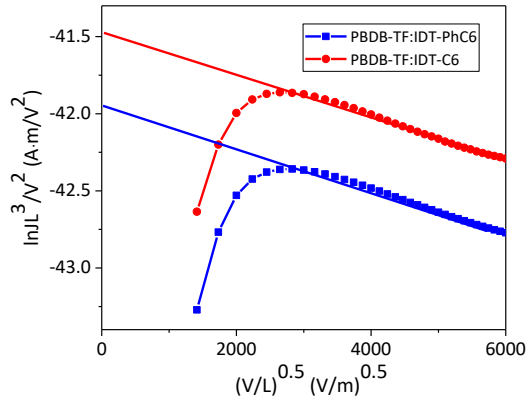


Figure S9. Hole mobility plots for PBDB-TF:IDT-C6 and PBDB-TF:IDT-PhC6 devices.

S10. Morphology of blended films

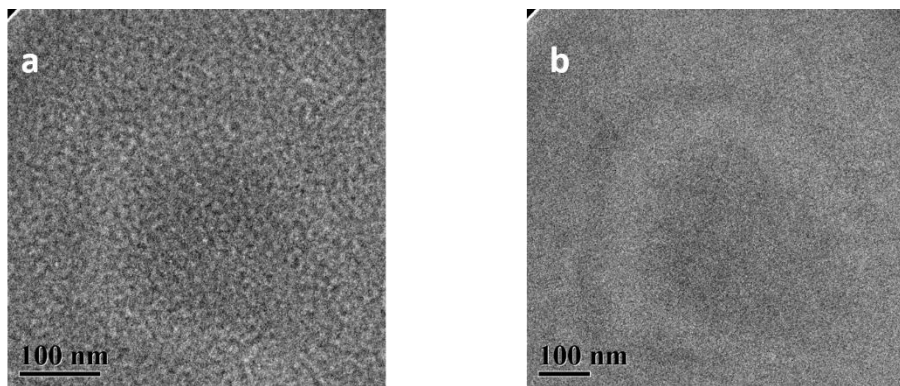


Figure S10. TEM phase image of a) PBDB-TF:IDT-C6 blended films. b) PBDB-TF:IDT-PhC6 blended films.

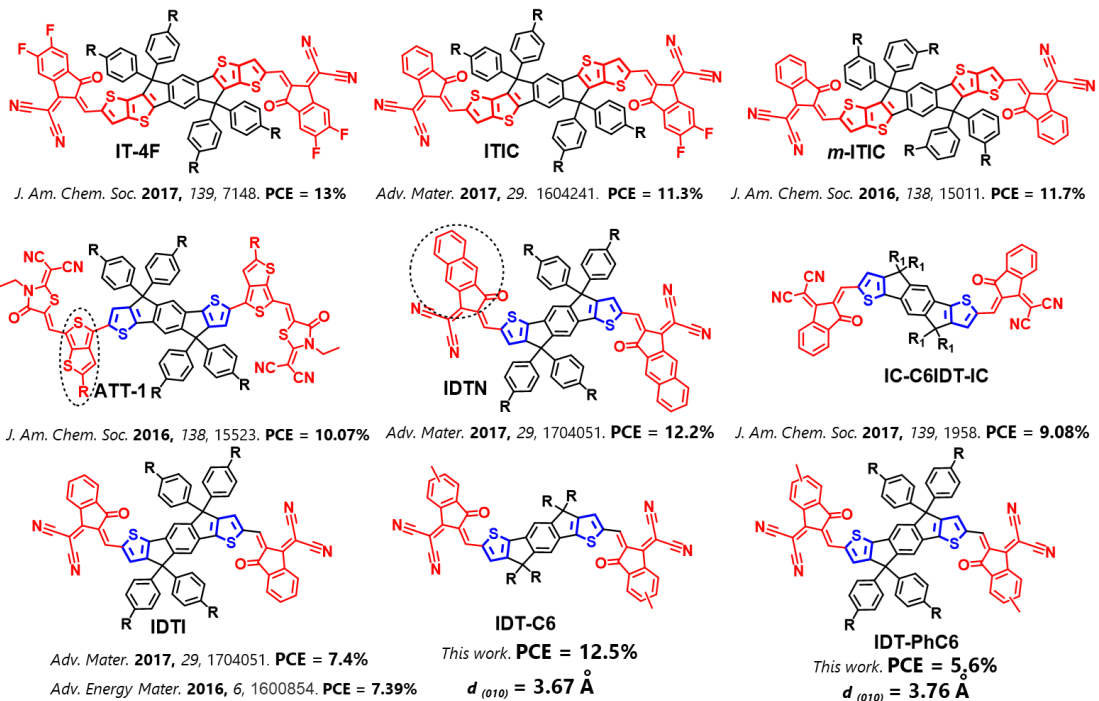


Figure S11. Chemical structures of typical acceptors with hexyl or hexylphenyl side chains.

References

- 1 G. G. Malliaras, J. R. Salem, P. J. Brock and C. Scott, *Phys. Rev. B*, 1998, **58**, R13411.
- 2 S. Züfle, S. Altazin, A. Hofmann, L. Jäger, M. T. Neukom, T. D. Schmidt, W. Brütting and B. Ruhstaller, *J. Appl. Phys.*, 2017, **121**, 175501.